Efficiency of employing fiber-based finite-length plastic hinges in simulating the cyclic and seismic behavior of steel hollow columns compared with other common modelling approaches

Mojtaba Farahi[†] and Saeed Erfani[‡]

Department of Civil Engineering, Amirkabir University of Technology, Tehran, Iran

Abstract: The accuracy and efficiency of the modelling techniques utilized to model the nonlinear behavior of structural components is a significant issue in earthquake engineering. In this study, the sufficiency of three different modelling techniques that can be employed to simulate the structural behavior of columns is investigated. A fiber-based finite length plastic hinge (FB-FLPH) model is calibrated in this study. In order to calibrate the FB-FLPH model, a novel database of the cyclic behavior of hollow steel columns under simultaneous axial and lateral loading cycles with varying amplitudes is used. By employing the FB-FLPH model calibrated in this study, the interaction of the axial force and the bending moment in columns is directly taken into account, and the deterioration in the cyclic behavior of these members is implicitly considered. The superiority of the calibrated FB-FLPH modelling approach is examined compared with the cases in which conventional fiber-based distributed plasticity and concentrated plasticity models are utilized. The efficiency of the enumerated modelling techniques is probed when they are implemented to model the columns of a typical special moment frame in order to prove the advantage of the FB-FLPH modelling approach.

Keywords: cyclic behavior; seismic behavior; fiber-based finite-length plastic hinge model; fiber-based modelling techniques; cyclic strength deterioration; axial force-bending moment interaction

1 Introduction

Predicting and assessing the seismic behavior of different types of structures and structural elements is of key importance in performance-based earthquake engineering (Fenves and McKenna, 2007; Freeman, 2000). Consequently, there is an inevitable demand for simulating the behavior of structural lateral load resisting systems when these systems are subjected to ground motions. The uncertainties involved in the decision making procedure, as a part of performance-based earthquake engineering, depends on the accuracy of such numerical simulations. The accuracy of the results of these simulations depends on the accuracy of the modelling techniques which are employed to numerically model the behavior of different structural components. Hence, a significant attempt has been made by different researchers in order to develop and calibrate reliable and computationally efficient numerical modelling approaches for different structural elements.

The modelling approaches suggested for structural elements can be categorized into three groups, including phenomenological models, beam-column elements with distributed plasticity formulation and three dimensional continuum finite element models. Phenomenological models are the simplest and most computationally efficient type of numerical models (Ikeda *et al.*, 1984; Khatib *et al.*, 1988). In this type of models, a predefined hysteretic behavior describes the nonlinear behavior of the intended structural elements. This hysteretic behavior should be first defined and calibrated based on available experimental observations. However, a comprehensive experimental database is only available for limited types of structural members. Hence, the results of this kind of modelling are only reliable for restricted types of structural members and for a limited range of cyclic or seismic behavior. Meanwhile, different techniques have been employed to physically model the behavior of structural elements using beam-column elements. For example, Hall and Challa (1995) discretized the cross-section of members to fiber elements in order to describe the inelastic hysteretic response of steel members. This type of modelling was improved by other researchers in order to take into account the interaction between bending moment and axial force (Jin and El-Tawil, 2003; Uriz *et al.*, 2008). Continuum finite element method is used in the third category of modelling approaches that

Correspondence to: Saeed Erfani, Department of Civil Engineering, Amirkabir University of Technology, Tehran, Iran
Tel: (+98) 2164543086
E-mail: sderfani@aut.ac.ir
[†]PhD Candidate; [‡]Assistant Professor

is employed in earthquake engineering applications. The nonlinear behavior of individual structural members can be predicted with sufficient accuracy when using this approach (Fu, 2009; Imanpour *et al*., 2016; Miyamura *et al*., 2015). However, this type of modelling approach is not commonly used for simulating the behavior of an entire structure because of its complexity and computational expense.

Columns are one of the main structural members in buildings and their lateral load resisting frames. Consequently, the accuracy of the numerical simulations conducted on buildings and these frames depends directly upon the accuracy of the modelling techniques used to capture the nonlinear behavior of columns. Previous experimental studies have shown that the cyclic behavior of steel columns depends upon geometric and material properties of these members (Cheng *et al*., 2013; Kanvinde *et al*., 2014; Nakashima and Liu, 2005; Ucak and Tsopelas, 2014). The initial strength of steel columns deteriorates during a cyclic or seismic loading mainly due to the local geometric instabilities (Lignos and Krawinkler, 2009; Nakashima and Liu, 2005). The rate of this deterioration in the cyclic behavior of steel columns is more severe for columns with large local slenderness (large width to thickness ratio) (Lignos and Krawinkler, 2009). Accordingly, the modelling technique that is employed to simulate the behavior of steel columns should be capable of representing the deterioration in the cyclic behavior of these members. In addition, the columns of lateral load resisting systems are generally subjected to two simultaneous structural demands, which distinguishes them from other structural members. During severe ground motions, a significant level of axial force demand is developed in the columns of lateral load resisting frames in conjunction with a high nonlinear flexural demand. Hence, the interaction between the axial force and the bending moment (P-M interaction) should be taken into account as the seismic and cyclic behavior of these members is numerically simulated.

Any model from the aforementioned categories of modelling approaches can be implemented in order to simulate the seismic and cyclic behavior of column members in steel structures. Employing fiber-based finite length plastic hinges (FB-FLPH) at the ends of column members is the most recent modelling approach that has been utilized to simulate the seismic behavior of these members (Hamidia *et al*., 2014; Tzimas *et al*., 2016; Farahi and Erfani, 2017). Further details about this modelling approach has been discussed in this paper. In addition, a stress-strain constitutive model has been calibrated in this research such that the seismic behavior of square hollow steel sections can be reasonably simulated by assigning this material model to the fiber elements. The FB-FLPH model calibrated and used in this study accounts for both P-M interaction and the deterioration in the cyclic behavior of these members.

However, the FB-FLPH model has not yet been implemented widely in the literature. Hence, the accuracy and the efficiency of this model has tentatively been compared with two other prevalent modelling approaches. In one of these approaches, concentrated plastic hinges (CPH) are used and it is referred to as the CPH model. The nonlinear behavior of columns is assumed to be concentrated at zero-length end hinges in this model. In the other model compared with the intended FB-FLPH model in this research, the cross-section of column members is discretized to nonlinear fiber elements along the entire length of these members. This approach is referred as fiber-based distributed plasticity (FB-DP) model. These modelling techniques are discussed in detail in the next section of this paper.

In the next step, it has been investigated how the results of time-history analysis conducted on structural moment frames can be affected if the FB-FLPH model calibrated in this study is used to simulate the seismic behavior of their columns. Hence, all the mentioned models have been employed to model the columns of a special moment frame. The numerical models provided for the frame were analyzed next under numerous ground motion records with different increasing intensities. The time-history results of these analyses were eventually utilized to assess the efficiency of the FB-FLPH model compared with the two other prevalent models.

2 Different numerical models implemented to simulate the nonlinear behavior of columns

Among different modelling techniques employed by various researchers to simulate the seismic behavior of steel column members, three major techniques can be distinguished. Implementing concentrated plastic hinges at the ends of members, discretizing the cross-section of members to nonlinear fiber elements, and utilizing fiber-based finite-length plastic hinges can be enumerated as the prevalent methods for modelling the nonlinear behavior of steel column members. In this study, all the mentioned methods have been employed to simulate the cyclic and seismic behavior of different square hollow steel sections in order to highlight the merits and the deficiencies of these modelling methods. More details about the modelling techniques specifically employed in this study are explained in the following sections. The required numerical simulations have been conducted utilizing the OpenSees simulation platform in this study. Hence, the following subsections also describe how each modelling technique has been employed using the modelling features of this simulation platform.

2.1 Concentrated plastic hinge (CPH) model

The concentrated plasticity model developed by Lignos and Krawinkler (2011) was chosen in this study in order to represent the phenomenological modelling approach. This model was also calibrated in order to

simulate the cyclic behavior of hollow steel columns based on the available experimental results (Lignos and Krawinkler, 2009). The main focus is on the flexural behavior of columns in this model. According to this modelling approach, zero-length plastic hinges at both ends of the columns represent the nonlinear behavior of these members. Lignos and Krawinkler (2009) have improved this modelling technique in order to implicitly account for the cyclic deterioration in the seismic and cyclic behavior of column members. The behavior of the end plastic hinges is determined by the uniaxial material assigned to the section of these zero-length hinges. A trilinear backbone specifies the strength bound for the material model employed by Lignos and Krawinkler (2011). Figure 1 shows the parameters which are required to define the behavior of the mentioned material model. The yield capacity and the elastic stiffness of each member can be determined based on its material properties. In addition, Lignos and Krawinkler (2009) suggested the following equations to assess the plastic rotation capacity (θ_p) and post-capping rotation capacity (θ_pc). These equations were derived based on the regression analysis conducted by these researchers using an experimental database for steel columns. Equation (1) and Eq. (2) relate θ_p and θ_pc to the local slenderness, axial force ratio, and material properties of each column. The ratio of the width to the thickness of each member (d/t) represents the slenderness, while the axial force ratio is defined as the ratio of the presumed axial force in each column (N) to its nominal axial yield capacity (N_y). Note that all the following equations are valid

for $0 \le \dfrac{N}{N_\mathrm{y}} \le 0.4$, $20 \le \dfrac{d}{t} \le 40$, $270 \le F_\mathrm{y} \le 460$ MPa (Lignos and Krawinkler, 2009).

$$\theta_\mathrm{p} = 0.614 \left(\frac{d}{t} \right)^{-1.05} \left(1 - \frac{N}{N_\mathrm{y}} \right)^{1.18} \left(\frac{c \cdot F_\mathrm{y}}{380} \right)^{-0.11} \quad (1)$$

$$\theta_\mathrm{pc} = 13.82 \left(\frac{d}{t} \right)^{-1.22} \left(1 - \frac{N}{N_\mathrm{y}} \right)^{3.04} \left(\frac{c \cdot F_\mathrm{y}}{380} \right)^{-0.15} \quad (2)$$

In the above equations, c is the unit conversion factor and depends on the unit that is chosen for material properties. It is equal to 1 if MPa is used, and a unit conversion factor $c = 6.895$ should be applied if material yield stress (F_y) is chosen in ksi (Lignos and Krawinkler, 2009). It can be inferred from Eq. (1) and Eq. (2) that increasing the presumed axial force demand on columns results in smaller plastic rotation capacity and steeper post-capping. In addition, smaller plastic rotation capacity and post-capping rotation capacity are expected for steel sections with higher slenderness (width to thickness ratio).

Furthermore, the initial strength and stiffness of the mentioned material model can be deteriorated during cyclic loading. The rate of this deterioration depends on a parameter named the cyclic deterioration parameter (Λ). Similarly, another equation was suggested for evaluating this parameter (Eq. (3)) (Lignos and Krawinkler, 2009). Choosing smaller values for Λ results in more deterioration in the cyclic behavior of the column members. According to Eq. (3), smaller Λ values are suggested for columns with more slenderness and the columns under larger axial loading. It has experimentally been proved that severe deterioration can be expected for such columns due to the early occurrence of local buckling (Kawaguchi and Morino, 2001; Kurata *et al.*, 2005; Nakashima and Liu, 2005).

$$\Lambda = 3012 \left(\frac{D}{t} \right)^{-2.49} \left(1 - \frac{N}{N_\mathrm{y}} \right)^{3.51} \left(\frac{c \cdot F_\mathrm{y}}{380} \right)^{-0.2} \quad (3)$$

According to the experimental database used by Lignos and Krawinkler (2009) to calibrate this material model, the rate of cyclic deterioration becomes negligible after a certain level of strength reduction. Hence, they
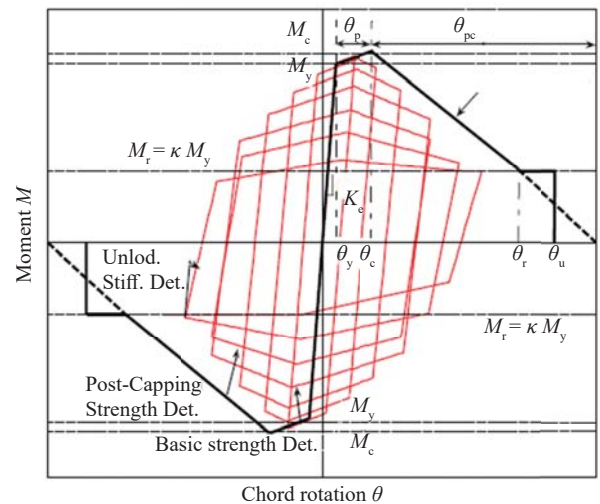
$M_\mathrm{y}, \theta_\mathrm{y}$: Effective yield strength and rotation

K_e: Effective Stiffness

$M_\mathrm{c}, \theta_\mathrm{c}$: Capping Strength and associated rotation for monotonic loading

θ_p: Pre-capping rotation capacity for monotonic loading

θ_pc: Post-capping rotation capacity

M_r: Residual Strength

θ_u: Ultimate Rotation capacity

Fig. 1 Modified Ibarra-Krawinkler deterioration model for simulating the cyclic behavior of steel hollow columns (Lignos and Krawinkler, 2011)

considered a residual capacity for members that can be introduced to the model by a parameter called the residual strength ratio, κ (Fig. 1). The value of 0.25 that was suggested for this modelling parameter (Lignos and Krawinkler, 2009) has been used in this study.

In order to implement this modelling approach in OpenSees, zero-length elements can be used to model the plastic hinges at the ends of each column member, and elastic beam-column elements can be employed to model column members between the end hinges. The stiffness of the hinges as well as the stiffness of the internal elastic part is assigned such that the elastic stiffness of the intended column member is retrieved (Lignos and Krawinkler, 2011). A uniaxial material known as "Bilin" material from the uniaxial material library from the OpenSees simulation platform is assigned to the section of the zero-length elements. The behavior of this material is ruled based on the material model discussed in this section (Lignos and Krawinkler, 2011). The required parameters to define "Billin" material model were evaluated based on the above equations suggested by Lignos and Krawinkler (2011).

Employing the mentioned modelling technique can facilitate the modelling procedure due to its simplicity. Moreover, it can dramatically expedite the numerical simulations because the nonlinear behavior of columns is limited to zero-length hinges only at the ends of these members. However, this model is mainly developed to simulate the nonlinear flexural behavior of column members. That is, the P-M interaction is not explicitly taken into account. In addition, the mentioned moment-rotation constitutive law applied as the behavior of end plastic hinges was calibrated based on limited experimental data. A comprehensive experimental database has not been developed for all types of structural columns, and almost all the experiments have been conducted under loading scenarios that cannot accurately represent the seismic demands on columns. Most of the experiments conducted on column specimens have been performed under a constant level of axial loading in conjunction with lateral loading cycles, while both axial and flexural demands on columns fluctuate during a ground motion.

2.2 Fiber-based distributed plasticity (FB-DP) model

Beam-column elements with distributed plasticity formBeam-column elements with distributed plasticity formulation can be used to represent the seismic behavior of columns. In this method, the cross-section of column members is discretized to nonlinear fiber elements along their length. The nonlinear behavior of the fiber elements is governed by a constitutive stress-strain model. Accordingly, integrating the stress of all the fiber elements across any section cut along the intended member results in the resistance internal actions (axial force and bending moment) (Uriz et al., 2008). Figure 2 schematically presents this modelling technique.

In order to employ the FB-DP model in this study,

columns were modeled with nonlinear beam-column elements in the OpenSees simulation platform, and the cross section of these elements were discretized to nonlinear fibers. Different patterns are available in this software for discretizing the cross-section of a member to fiber elements according to its geometry. Both force-based and displacement-based formulations can be applied using the nonlinear beam column elements in OpenSees. Nonlinear beam-column elements with displacement-based formulation were employed in this study to evade convergence problems and expedite the simulations. However, the displacement interpolation function of a displacement-based element can deviate from the exact solution. Hence, columns were divided into eight individual elements along their length in order to prevent any significant solution error (Karamanci and Lignos, 2014; Salawdeh and Goggins, 2013). A uniaxial bilinear material model which is known as "Steel02" in the uniaxial material library of the OpenSees simulation platform was assigned to the fiber elements across the section of all column members. This material model was initially suggested by Menegotto and Pinto (1973), and it was then modified to considered kinematic and isotropic hardening and implemented in the OpenSees simulation platform by Fillippou et al. (1983). The overall behavior of this material is defined by specifying the material yield stress, F_y, the elastic modulus, E, and the strain-hardening ratio, b. The yield strength and elastic modulus can easily be assessed based on the material properties of the steel used to fabricate the intended columns. Strain-hardening ratio (the ratio of post-yield tangent to initial elastic tangent) has been considered equal to 0.02 in this study (Bosco et al., 2015; Eletrabi and Marshall, 2015). Three parameters ($R0$, $cR1$ and $cR2$) should also be evaluated to determine the transition from the elastic to the plastic branch of "Steel02" material model. In addition, four other parameters ($a1$, $a2$, $a3$, $a4$) are required to define the isotropic hardening behavior of this material model. Default values used for these parameters by the software were utilized for all of these parameters in this study.

In this modelling technique, the nonlinear behavior is not restricted only to the ends of the members. Employing this modelling approach also makes it possible to explicitly account for the interaction between the axial force and the bending moment in columns. Furthermore, the probable plastic elongation of columns is also captured as this method is used to simulate the
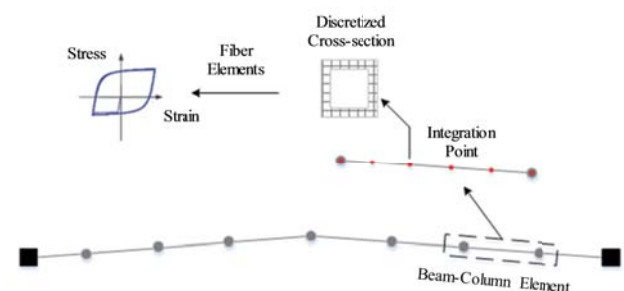

Fig. 2 Description of fiber-based distributed plasticity model

nonlinear behavior of columns. However, this modelling approach involves more computational efforts compared with the cases in which plastic hinges are employed. Another disadvantage is that the FB-DP model does not account for the inevitable deterioration in the cyclic behavior of steel columns.

2.3 Fiber-based finite length plastic hinge (FB-FLPH) model

Another fiber-based modelling technique has been introduced more recently to simulate the nonlinear behavior of steel column members. In this modelling approach, the nonlinear behavior is only attributed to the end parts of the column, which distinguished this modelling approach from the conventional distributed plasticity formulation. Hence, this numerical model for column members is known as the fiber-based finite-length plastic hinge (FB-FLPH) model. In this modelling approach, the cross-section of the columns is discretized to nonlinear fiber elements along the plastic hinges at the ends of these members. The behavior of the rest of the column members is assumed to be linear. The assumed distribution of the nonlinearity along the column members is consistent with what happens along these structural members of moment frames during severe lateral loading.

Since the distributed plasticity formulation is employed along the end plastic hinges, the P-M interaction in the intended column member as well as the probable plastic axial elongation is directly considered in this modelling approach. In addition, the probable deterioration in the hysteretic behavior of column members is also implicitly considered by assigning a uniaxial material model with varying strength bounds to the fiber elements. Hence, in contrast to the other mentioned modelling techniques, both critical aspects of a column cyclic behavior are taken into account as the FB-FLPH model is used to simulate the nonlinear behavior of that column.

2.3.1 Strain-stress constitutive model assigned to the fiber elements

The stiffness and strength deterioration options are available for the "Bilin" material model from the uniaxial material library of the OpenSees simulation platform. The deterioration rate in this material model is determined implementing the rule suggested by Ibarra *et al.* (2005). According to this rule, a reference hysteretic energy dissipation capacity is attributed to each member. During the modelling process, the reference hysteretic energy dissipation capacity of each member is calculated based on the value that is chosen for a modelling parameter. This modelling parameter is known as the deterioration parameter (Λ). The rate of the strength and stiffness deterioration in each exertion is then determined based on the energy dissipated in the previous exertion and the reference hysteretic energy dissipation capacity assumed for the intended member. Since selecting a large deterioration parameter results in

a large reference hysteretic energy dissipation capacity, the cyclic deterioration rate will be less for the cases in which larger values are selected for Λ. The mentioned uniaxial material model was originally developed in order to represent the moment-rotation relationship at the cross-section of structural elements; however, it is used in this study as a stress-strain relationship model that is assigned to the fiber elements. The key required parameters to define "Bilin" material model for the intended purpose in this study (except the deterioration parameter) are shown in Fig. 3. E_0, a_{sh}, and σ_y represent the initial stiffness, strain hardening ratio and the yielding strength, respectively. These parameters can be evaluated based on the material properties of columns. Eventually, the strength boundary for the constitutive strain-stress relationship can be defined by specifying appropriate values for ε_p (pre-capping plastic strain) and ε_{pc} (post-capping plastic strain) in conjunction with the aforementioned parameters. Hence, the intended material model should be first calibrated to find the most appropriate values for ε_p, ε_{pc}, and Λ.

2.3.2 Integration method

Since the intended model is a fiber-based model, it is necessary to implement an integration method as a part of the distributed plasticity formulation to calculate the element forces based on the section resultant forces at integration points (Hall and Challa, 1995). In general force-based distributed plasticity formulations, the inelasticity is tracked along the entire length of the intended member. If a strain-hardening constitutive model is assigned to the fiber elements, different integration methods with a different number of integration points can be selected in this formulation based on the required precision. However, in case of using a strain-softening constitutive relation, the behavior of the fiber elements follows the softening path only at one integration point in order to maintain the equilibrium. Hence, the results in that case depend on the weight of the integration point at which the softening behavior is captured. That is, different convergent results are obtained by choosing different numbers of integration points, and the general distributed plasticity models lose the objectivity as a strain-softening constitutive material model is used. This
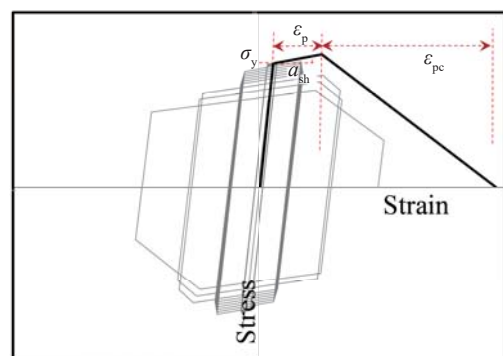

Fig. 3   Strength backbone of the material model used in fiber-based FLPH model

issue has been addressed as localization in the literature (Coleman and Spacone, 2001). Choosing an appropriate weight for the integration in which the softening has happened is an effective solution for the localization issue (Scott and Fenves, 2006). The appropriate integration weight should represent the length of the physical plastic hinge that forms in the intended member. As discussed in the following section, the length of the fiber-based finite-length plastic hinges has been chosen in this study based on the length of the plastic hinges that are expected to form at the ends of hollow steel columns. There are different special integration methods available in the OpenSees simulation platform that prescribe certain integration weights at the member ends. Among these plastic hinge integration methods, the regularized hinge integration method proposed by Scott and Hamutcuoglu (2008) has been employed in this study.

2.3.3 Length of end plastic hinges

An appropriate and realistic length should be chosen for the plastic hinges as the FB-FLPH modelling approach is used to simulate the nonlinear behavior of columns. In the experiments conducted on hollow steel columns, it has not been common to measure the length of columns in which the section of these members behaved nonlinearly. However, Denavit *et al.* (2015) measured the length of columns with nonlinear curvature as the length of plastic hinges during the experiments they conducted on concrete-filled tubular columns. According to the results of these experiments, they also suggested an analytical method to obtain the probable length for the plastic hinges at the ends of columns. This method has been utilized in this study to estimate the length of the plastic hinges formed at the ends of hollow steel columns.

If an example case of a cantilever column subjected to simultaneous axial and lateral loading is considered, the same bending moment and curvature distribution as that shown in Fig. 4 is expected along the intended column. Hence, the length of the plastic hinge (L_p) developed at the end of the intended column can be calculated based on the values of the maximum bending moment at the end of the column (M_u) and the yield bending moment (M_y) of the cross-section (Denavit *et al.*, 2015).

$$\frac{L_p}{L_0} = 1 - \frac{M_y}{M_u} \qquad (4)$$

In this study, the behavior of the selected HSS column samples was numerically simulated in ABAQUS under the loading protocol shown in Fig. 4. In addition to an increasing monotonic lateral load, the column samples were subjected to two levels of constant axial loading equal to 10% and 30% of the axial yield capacity of the cross-section of these columns. In this study, M_u was defined as the ultimate moment tolerated by the HSS specimens and M_y was identified as the bending moment

at which the yield stress was reached in any point of the intended columns. As M_u and M_y were evaluated for all the column specimens, Eq. (4) was used to calculate the length of plastic hinges formed in these columns. The results of these calculations are summarized in Tables 1 and 2. These tables reports the ratio of the plastic hinge length (L_p) to the length from the point of maximum moment to the inflexion point (L_0) for all the chosen HSS samples.

It can be inferred from Tables 1 and 2 that the length of plastic hinges formed in hollow steel columns decreases slightly as the local slenderness of these members increases. In addition, by increasing the level of axial loading, the length of the plastic hinges formed in columns is reduced. These correlations can be justified if it is noted that the increase in the local slenderness or the level of the axial load intensifies the concentration of the local effects in columns. However, L_p/L_0 was obtained in the limited range of 12%-24% for the HSS specimens as they were subjected to an axial load equal to 10% of their axial yield capacity. On the other hand, the values calculated for L_p/L_0 only vary between 13%-22% as the column specimens were subjected to an axial load equal to 30% of their axial yield capacity. Hence, L_p/L_0 has roughly been assumed as equal to 15% in this study since the length of plastic hinges formed in the different column archetypes was not significantly affected by the geometry and the material properties of these members.

2.3.4 Calibrating FB-FLPH modelling approach

In the most of the past studies regarding the cyclic behavior of hollow steel columns, these members were subjected to lateral loading cycles in conjunction with a constant level of axial loading. However, a novel database of the cyclic behavior of hollow steel columns was used in this study to calibrate the chosen material model instead of using the available experimental results. In order to develop this database, the behavior of several hollow steel columns were simulated in ABAQUS under a dual loading protocol that has been previously developed by the authors (Farahi and Erfani, 2017). This dual loading protocol consists of both cycles
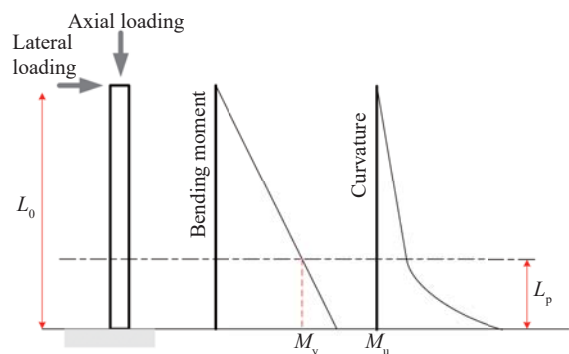

Fig. 4 Distribution of the bending moment and curvature along a cantilever column under simultaneous axial and lateral loading (Denavit *et al.*, 2015)

Table 1   Normalized length of plastic hinges (L_p/L_0) formed in the column samples as they were subjected to lateral increasing load in conjunction with a constant axial load equal to 10% of their axial yield capacity

	Type of Steel material	
	ASTM A500 Grade D	ASTM A500 Grade C
HSS 12×12×5/8	0.245	0.170
HSS 14×14×5/8	0.201	0.182
HSS 16×16×5/8	0.165	0.140
HSS 18×18×5/8	0.158	0.123
HSS 20×20×5/8	0.144	0.146

Table 2   Normalized length of plastic hinges (L_p/L_0) formed in the column samples as they were subjected to lateral increasing load in conjunction with a constant axial load equal to 30% of their axial yield capacity

	Type of Steel material	
	ASTM A500 Grade D	ASTM A500 Grade C
HSS 12×12×5/8	0.218	0.183
HSS 14×14×5/8	0.175	0.157
HSS 16×16×5/8	0.158	0.135
HSS 18×18×5/8	0.150	0.131
HSS 20×20×5/8	0.143	0.140

of lateral and axial loading with varying amplitudes. The amplitude and the fluctuation rate of these loading cycles were determined based on the range and the variation of the axial force and the lateral drift demands on the columns of various special moment frames when these frames were subjected to numerous ground motion records. These frames were chosen from 3, 6 and 10-story buildings with different plan configurations (Farahi and Erfani, 2016). Figure 5 shows the lateral and axial loading cycles of the intended dual loading protocol. Hence, the constitutive model in this study has been calibrated based on the cyclic behavior of several hollow steel column samples under the mentioned dual loading protocol so that the calibrated model can next be used to simulate the seismic behavior of these columns with a reasonable accuracy.

The column samples were selected from standard square hollow structural sections (HSSs) in order to develop the required database for the calibration process. The HSSs chosen as the column samples and their geometric properties are listed in Table 3. According to this table, the width to thickness ratio of the chosen column samples varied in the range of 17 to 30. Additionally, it was assumed that the column samples were fabricated from ASTM A500 Grade C and Grade D steel material. The yield strength of these types of steel material is equal to 345 MPa (50 ksi) and 248 MPa (36 ksi), respectively. The strain hardening ratio for both types of steel was assumed as equal to 0.5%. The height of all the column samples was chosen equal to 4000 mm. The behavior of the intended column

samples were next simulated under the simultaneous axial and lateral loading cycles presented in Fig. 5. In these simulations, the translational degrees of freedom (DOF) were constrained at one end and the rotational DOF were constrained at both ends of the columns. Note that the capability of the finite element simulations to predict the cyclic behavior of hollow steel columns has
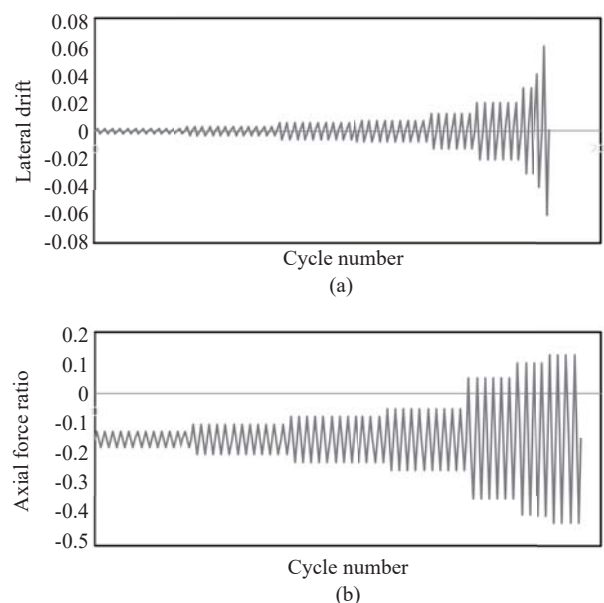

Fig. 5   (a) Lateral and (b) axial loading cycles of the dual loading protocol used in this study (Farahi and Erfani, 2016)

Table 3 Geometric properties of the sections of the chosen column samples

Hollow structural section	Nominal width (mm)	Thickness (mm)	Width to thickness ratio
HSS 12×12×5/8	305	15.9	17.7
HSS 14×14×5/8	356	15.9	21.1
HSS 16×16×5/8	406	15.9	24.5
HSS 18×18×5/8	457	15.9	25.8
HSS 20×20×5/8	508	15.9	29

previously been verified by the authors, and the details of the modelling procedure in the ABAQUS simulation platform can be found in (Farahi and Erfani, 2017). The results of the simulations are shown in Figs. 6 and 7 in terms of the bending moment at the ends of the column samples with respect to the imposed lateral drift to these columns. The curves in these figures have been utilized as the benchmark database in order to calibrate the material model assigned to the fibers along the plastic hinges using the FB-FLPH modelling approach.

As the next step, the column samples were modelled in the OpenSees simulation platform employing the FB-FLPH modelling approach. As mentioned before, it was first necessary to calibrate the material model assigned to the fibers along the plastic hinges. That is, the most appropriate values should be found for the unknown modelling parameters (ε_p, ε_{pc}, and Λ). Hence, numerous trial simulations were conducted with different values

for these modelling parameters until the best match was captured between the simulation results obtained using OpenSees and FB-FLPH modelling approach and the benchmark database of the cyclic behavior of column samples obtained previously. The numerical models of the column samples were subjected to axial loading cycles in the same phase as the lateral loading cycles in order to develop a representative benchmark database of the cyclic behavior of hollow steel columns. Hence, one side of the cross-section of the column samples was always under less compression compared to the other side of the cross-section during loading. Consequently, the cyclic behavior obtained for the column samples is not symmetric as is apparent in Figs. 6 and 7. In order to account for this phenomena, larger strain hardening capacity (ε_p) was considered for the fiber elements in tension in the calibration procedure. According to the calibration results, the appropriate values obtained for
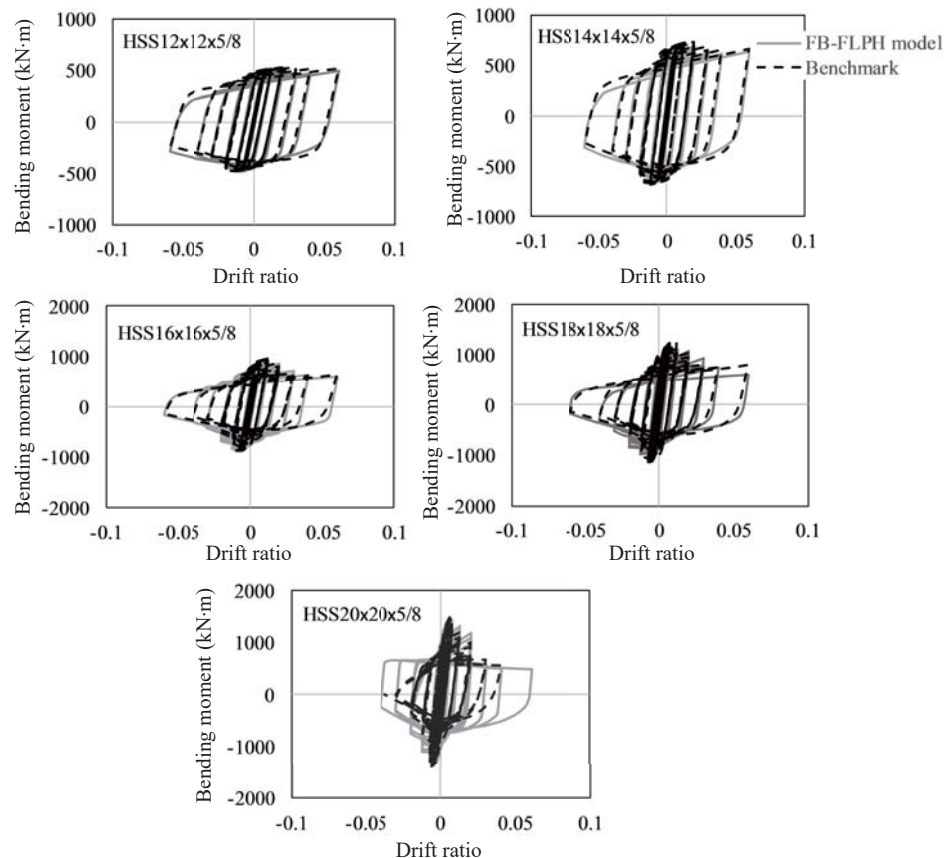
Fig. 6 End bending moment-lateral drift curves for the column samples fabricated from ASTM A500 grade D steel material
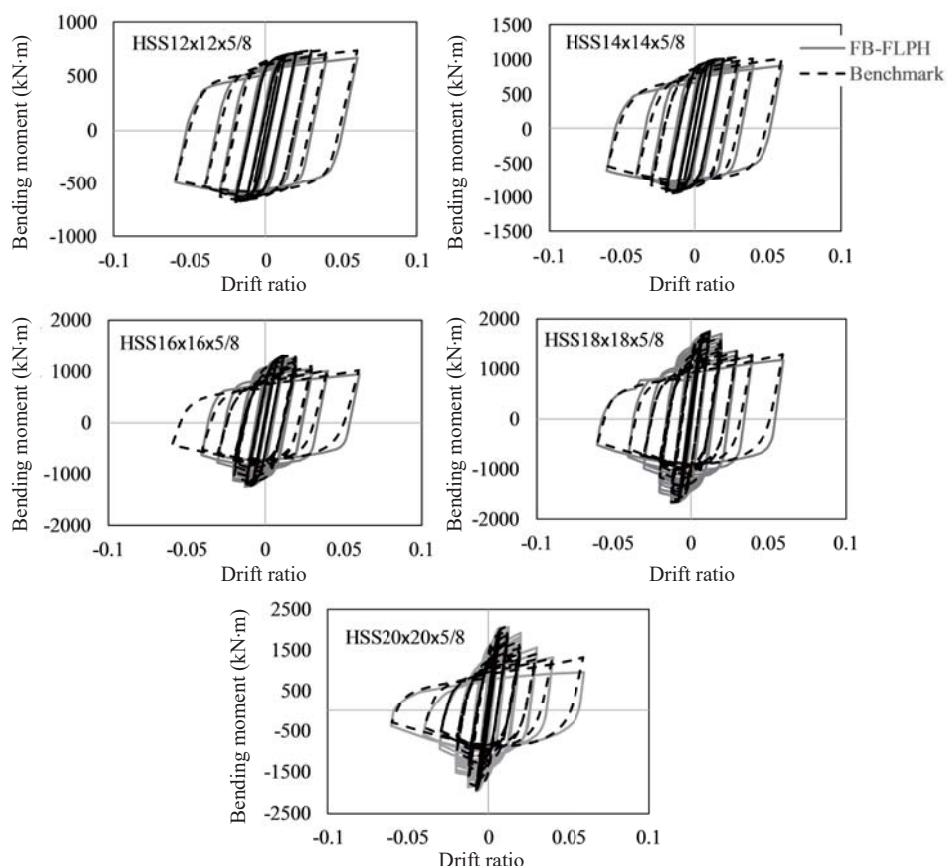
Fig. 7   End bending moment-lateral drift curves for the column samples fabricated from ASTM A500 grade C steel materia

ε_p and ε_{pc} were not dependent on the geometry and the material properties of the columns. Hence, in this study, ε_p and ε_{pc} were generally assumed as equal to 0.1 and 0.25 when the fiber elements are in tension and equal to 0.02 and 0.25 as the fiber elements are under compression. However, different values were assigned to Λ in order to simulate the deterioration in the cyclic behavior of different column samples since different rates of the deterioration were observed in the cyclic behavior of different column samples. The values of Λ that resulted in the most appropriate rate of deterioration in the cyclic behavior of the column samples are listed in Table 4. The cyclic behavior of the column samples simulated using the calibrated FB-FLPH modelling approach are also shown in Figs. 6 and 7.

According to Figs. 6 and 7, the benchmark database of the cyclic behavior of hollow steel columns provided in this study did not demand for considering a residual strength for the fiber elements as long as columns are subjected to drift ratios less than 0.06. Furthermore, the effect of employing different numbers of fiber elements across the section of columns was also investigated during the calibration procedure. Eventually, it was decided to use ten and three fiber elements along the length and through the thickness of the cross-sections of the column samples. According to the trial simulations, employing more fibers barely affected the simulation results, while it increased the time of the simulation. Figure 8 shows the results obtained for one of the column samples as the cross-section of the column was discretized to a different

Table 4   Appropriate values for the deterioration modelling parameter obtained for the column samples

	Type of Steel material	
	ASTM A500 Grade D	ASTM A500 Grade C
HSS 12×12×5/8	1.4	1.6
HSS 14×14×5/8	1.2	1.4
HSS 16×16×5/8	0.8	0.8
HSS 18×18×5/8	0.6	0.8
HSS 20×20×5/8	0.5	0.6

number of fiber elements along the end plastic hinges.

Lignos and Krawinkler (2009) investigated a comprehensive database of available experimental data and statistically proved that the rate of cyclic deterioration is significantly dominated by the width to thickness ratio and the material strength of the steel columns. According to this finding, a regression analysis has also been conducted in this study in order to develop a function that predicts an appropriate value for Λ based on the mentioned predictive variables. Equation (5) represents the function obtained from the multivariate linear regression analysis performed in this study. The coefficient of determination, R^2, was calculated as equal to 0.945 for the mentioned regression analysis. Hence, it can be concluded that the developed equation explains approximately 95% of the variability in the response variable Λ. Note that the suggested equation is obtained based on a limited database representing the cyclic behavior of steel hollow columns with a width to thickness ratio in the range of 17-30 and the steel material yield strength equal to 345 and 248 MPa. However, it is worth noting that web width to thickness ratio of any built up box-shaped sections that comply with the provisions of AISC 341-10 cannot exceed $1.12\sqrt{E/F_\text{y}}$ (27 and 32 for ASTM A500 grade C and D, respectively). Hence, the formulation is expected to be valid for all the hollow box-shaped sections that can be used as structural columns in seismic prone regions.

$$\Lambda = 14345 \cdot \left(\frac{d}{t}\right)^{-2.066} \cdot \left(\frac{E}{F_\text{y}}\right)^{-0.461} \qquad (5)$$

In this equation, d and t represent the width and the thickness of each column. E and F_y stand for the elastic modulus and the yield stress of the constitutive material of each column, respectively.
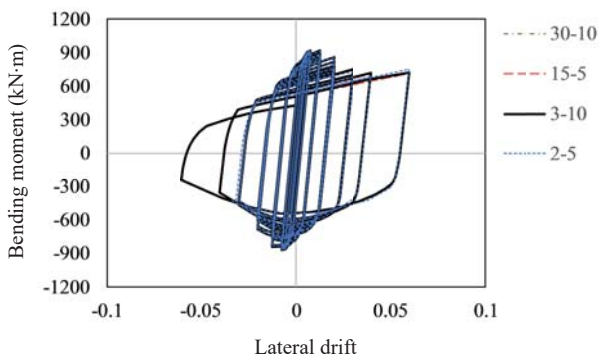

Fig. 8   Effect of employing different discretization patterns as FB-FLPH modelling approach was used to simulate the cyclic behaviourbehavior of HSS16 × 16 × 5/8 column sample (first and second number in the legend refers to the number of fiber elements along the length and through the thickness of the cross-section respectively)

3   Efficiency of the different modelling techniques in simulating the seismic behavior of columns as the members of steel moment frames

All the modelling techniques mentioned in the previous section were initially developed in order to simulate the nonlinear behavior of columns as the members of structural frames. Hence, introducing and employing any specific modelling technique for structural members can only be justified if it can improve the simulation of the seismic response of structural frames in terms of the accuracy or the computational expense. In this section, the efficiency of the three mentioned modeling techniques has been investigated as they were employed to model the column members of a steel special moment frame (SMF). It has been illustrated how the accuracy and the computational cost of the numerical simulations conducted on a sample SMF can be affected by using each of the mentioned models. Hence, the efficiency of the model calibrated in this study (FB-FLPH) has been investigated compared with the two other prevalent modelling approaches in the literature.

The SMF that has been chosen as the structural frame archetype in this study was one of the lateral load resisting frames of a 6-story building. The plan of this building is shown in Fig. 9, and the selected frame is highlighted in the plan view. The building was first loaded and designed according to ASCE/SEI 7-10 (2010) and AISC 360-10 (2010), respectively. Design of the lateral load resisting system (SMFs) of the building also complied with the seismic provisions of AISC 340-10 (2010). Figure 9 shows the results of the design procedure for the selected SMF archetype. The height of all the stories was considered as the same and equal to 3.5 m, except for the height of the first story, which was chosen as equal to 4 m. The dead load was chosen as equal to 4.0 kN/m² on the floors of the intended building. In addition, the values of 2.0 and 1.5 kN/m² were selected as the live loads on the floors and on the roof of the building, respectively. Column sections were chosen from HSS sections, and wide flange sections were assigned to the beam members. It was also assumed that all the sections were fabricated from the steel material of type ASTM A500 grade D.

Three different nonlinear models were provided for the selected 6-story 2-span SMF archetype. All the modelling details were the same in these three frame models except the modelling approach used to numerically simulate the structural behavior of column members. In each frame model, one of the techniques discussed in this study was used to model the columns of the SMF archetype. Hence, each frame model has been named based on the approach implemented to model its columns. For example, frame model CPH refers to the model of the SMF archetype in which concentrated
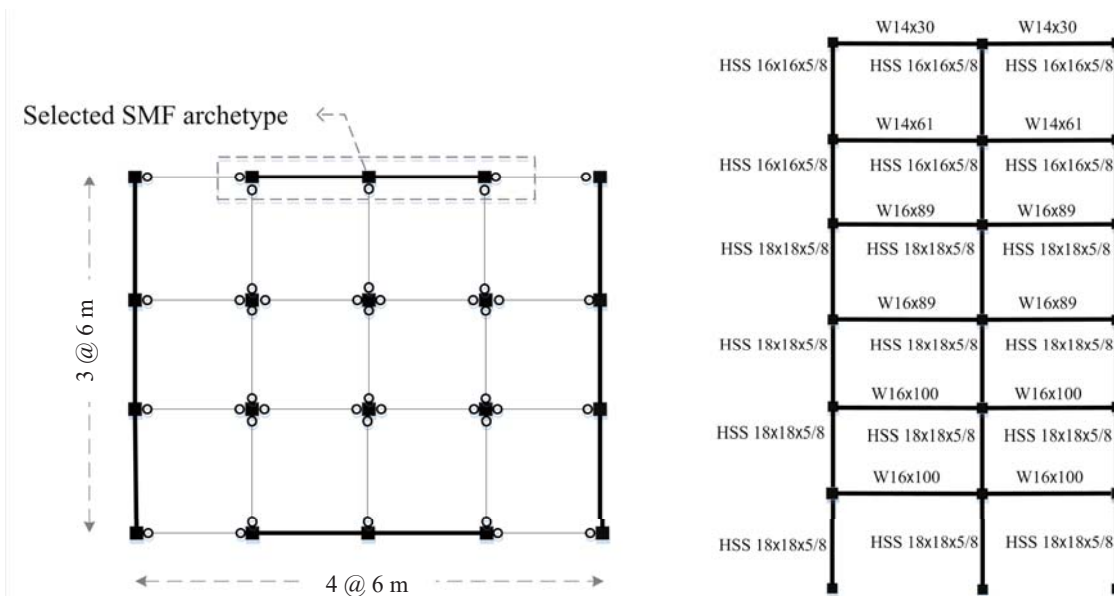
Fig. 9   Plan view of the selected building

plastic hinges were utilized to simulate the nonlinear behavior of the columns. The modelling procedure and the nonlinear dynamic analyzes were conducted utilizing the OpenSees simulation platform. The behavior of the numerical frame models were simulated under several ground motion records with different intensities and the time-history responses of these models were recorded. The results of the simulations were then post-processed and investigated in order to reveal more about the performance of the aforementioned modelling techniques in simulating the behavior of the columns as the critical members of the selected structural frame.

Three different modelling techniques were employed to model the columns of the chosen SMF were explained in detail in section 2. Note that the geometric and material properties of the column members of the designed frame are within the validity range of Eqs. (1)-(3) calibrated by Lignos and Krawinkler (2011) and Eq. (5) calibrated in this study. Furthermore, concentrated plastic hinges were employed to model the nonlinear behavior of the beams of the SMF archetype in all the frame models. Zero length elements were implemented to model the plastic hinges, while the beams between the end hinges were modelled with elastic beam-column elements. The elastic stiffness of the beams and the end hinges were modified such that the total stiffness of the system represents the elastic stiffness of the designed beams. The "Bilin" material model was assigned to the section of the zero-length elements to define the behavior of the end plastic hinges. As stated before, the strength of this material is limited to a trilinear bound. In addition, the initial stiffness and the ultimate strength of this material model can be deteriorated during cyclic and seismic loading. The formulations suggested by Lignos and Krawinkler (2011) were used to evaluate the required

modelling parameters of the "Billin" material model. These formulations were obtained through a calibration procedure and subsequent regression analysis conducted based on a comprehensive experimental database gathered for beam members (Lignos and Krawinkler, 2011).

As the three different numerical models were provided for the chosen SMF, the seismic response of these frame models were numerically simulated under numerous ground motion records. The inherent characteristics of the ground motion records were variant and diverse. Hence, it was decided to use a large number of ground motion records in order to evade bias and unconvincing conclusions. The far field ground motion record set introduced in FEMA P695 (2009) was used in this study. This set consists of 22 pairs of ground motion records which were introduced in Table 5. In addition, an ID number has been assigned to each record in this table.

The time-history analyses were conducted under each of the seismic records in the intended set with different intensities. That is, the intensity of each record was increased after each simulation and before conducting the next simulation using that record. This kind of dynamic analysis is known as incremental dynamic analysis (IDAs). The intensity of each seismic record for each simulation was determined by a scale factor multiplied to it before conducting the simulation. Two levels of scaling were applied on the record set according to FEMA P695 (2009). First, the records were normalized by their peak ground velocity. Thus, the unwarranted variability between the records was removed while preserving the variation between their frequency contents (FEMA, 2009). Second, the normalized records were collectively scaled to increasing ground motion intensities (FEMA, 2009; Farahi and Mofid, 2013). The

Table 5   Seismic records used in this study

Record ID	Earthquake name	Magnitude	Year
1, 2	Northridge	6.7	1994
3, 4	Northridge	6.7	1994
5, 6	Duzce	7.1	1999
7, 8	Hector Mine	7.1	1999
9, 10	Imperial Valley	6.5	1979
11, 12	Imperial Valley	6.5	1979
13, 14	Kobe	6.9	1995
15, 16	Kobe	6.9	1995
17, 18	Kocaeli	7.5	1999
19, 20	Kocaeli	7.5	1999
21, 22	Landers	7.3	1992
23, 24	Landers	7.3	1992
25, 26	Loma Prieta	6.9	1989
27, 28	Loma Prieta	6.6	1989
29, 30	Manjil	7.4	1990
31, 32	Superstition Hills	6.5	1987
33, 34	Superstition Hills	6.5	1987
35, 36	Cape Mendocino	7	1992
37, 38	Chi-Chi	7.6	1999
39, 40	Chi-Chi	7.6	1999
41, 42	San Fernando	6.6	1971
43, 44	Friuli	6.5	1976

scale factors in the second level represented the ratio of the spectral response acceleration of the input records at the fundamental period of the selected building (S_{aT}) to the maximum considered earthquake (MCE) spectral response acceleration for that fundamental period (S_{MT}). The fundamental period (T) of the 6-story building selected in this study has been calculated as equal to 1.14 s based on the formulation suggested in Chapter 12 of ASCE/SEI 7-10 (2010). For the selected building with the mentioned fundamental period, S_{MT} was evaluated as equal to 0.76 g (gravity acceleration) based on the acceleration response spectrum suggested in FEMA P695 (2009). The acceleration response spectra of the ground motion records used in this study, after the first level of scaling, are shown in Fig. 10. This figure also shows the MCE acceleration spectrum.

The main focus was placed on the interstory drift ratio time-histories among the different outputs that can be expected from the nonlinear dynamic analysis conducted in this study. There is a direct relation between the probability of side-sway collapse of common moment frames and the interstory drift ratios in these frames. Accordingly, this seismic demand has been mostly used in previous studies (Del Carpio *et al.*, 2016; FEMA, 2009; Karamanci and Lignos, 2014; Vamvatsikos and Cornell, 2002) and in this study in order to assess the seismic performance of lateral load resisting frames. Drift ratio

time-histories of all the stories of the three intended frame models were recorded during the simulations conducted in this section of the study. Figure 11 shows the story drift ratio time-histories obtained under records No. 5 and No. 29 at two levels of excitation. These drift time–histories were obtained for the story of the intended frame models in which the highest peak drift ratio was captured (under the relevant record with each intended intensity).   For the low-intensity excitations, when the response of the intended frame is in the elastic range, employing the three approaches for modelling the
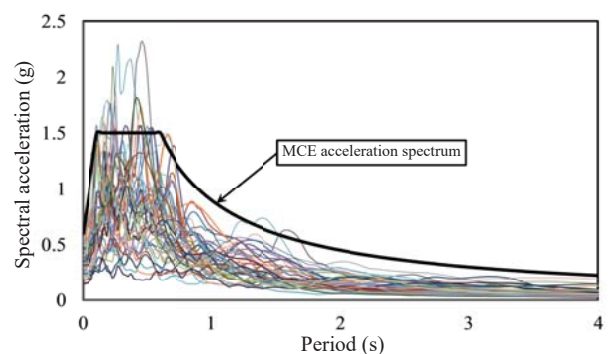

Fig. 10   Acceleration response spectra of the ground motion records utilized in this study in conjunction with the MCE acceleration response spectrum
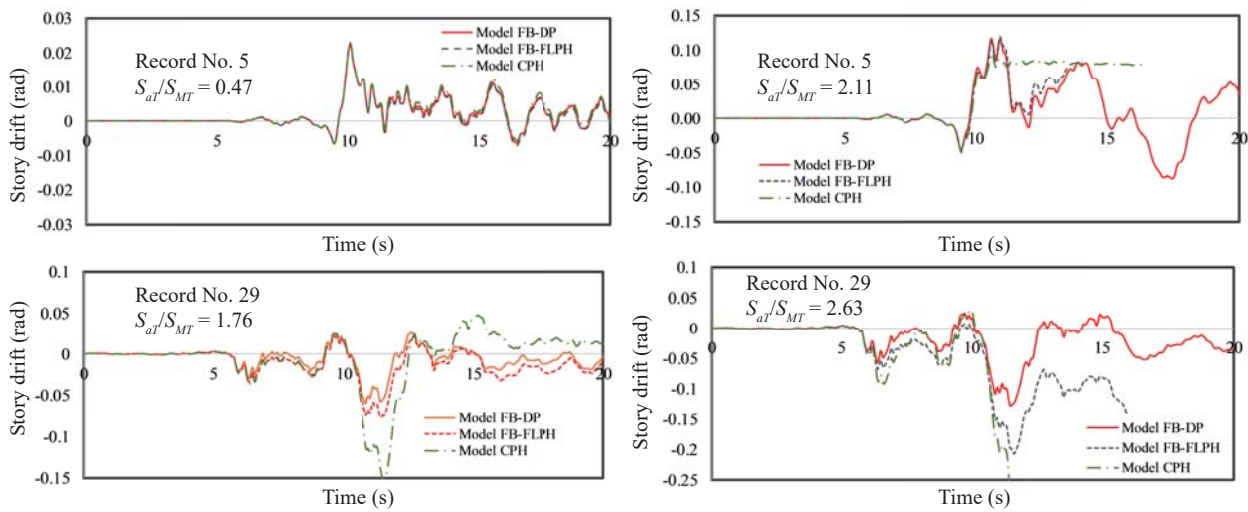
Fig. 11 Time-histories of maximum story drift ratios obtained from numerical simulations

columns resulted in the same time-histories. However, for higher intensities, implementing the FB-FLPH model resulted in higher maximum and residual story drift ratios compared with the case in which the columns of the SMF archetype were modelled with the conventional fiber-based distributed plasticity (FB-DP) method. This difference is due to the fact that the deterioration in the seismic behavior of columns caused by local buckling is implicitly taken into account as the FB-FLPH approach is utilized.

The simulations performed on the frame model CPH (the model in which concentrated plastic hinges were employed at the ends of the columns) were generally affected by numerical instabilities for higher seismic intensities. In addition, the results obtained for the frame model CPH notably deviated from the results obtained for the other frame models in the inelastic range. In order to define the concentrated plastic hinges, the required modelling parameters were calculated using the equations suggested by Lignos and Krawinkler (2009). These equations relate the modelling parameters to a constant level of axial load that is presumed to be developed in the intended columns. However, the axial force demand on the columns of a moment frame is not constant during a seismic event (Farahi and Erfani, 2016). In this study, three different constant levels of axial force, 10, 20 and 30% of the axial yield capacity of the columns, were assumed to calculate the required modelling parameters. However, the results presented in Fig. 11 were obtained assuming a constant level of axial force in columns equal to 20% of the axial yield capacity of these members. Figure 12 shows the story drift ratio time-histories that were obtained assuming the three mentioned constant levels of axial force in the columns to evaluate the modelling parameters. The time-history responses in this figure were recorded as frame model CPH was subjected to record No. 18 with two different intensities. It is apparent from this figure that

the results of the simulations were affected by the level of axial force presumed to be developed in the columns in order to evaluate the modelling parameters. However, it is not realistic to assume that the same level of axial force is developed in all the columns of a SMF and under different ground motions. This fact can be highlighted as one of the disadvantages of the CPH modelling approach.

The results of the incremental dynamic nonlinear analysis (IDAs) conducted on the three intended frame models are summarized as IDA curves shown in Fig. 13. Each curve represents the results of the nonlinear dynamic analysis performed under each individual ground motion record scaled to 20 different increasing intensities. Each point stands for each nonlinear dynamic analysis and the maximum story drift ratio, among all the stories, obtained from that analysis. Incremental dynamic analyses were utilized to establish the median collapse capacity, $\overline{S}_{CT}$, and consequently the collapse margin ratio, CMR, for
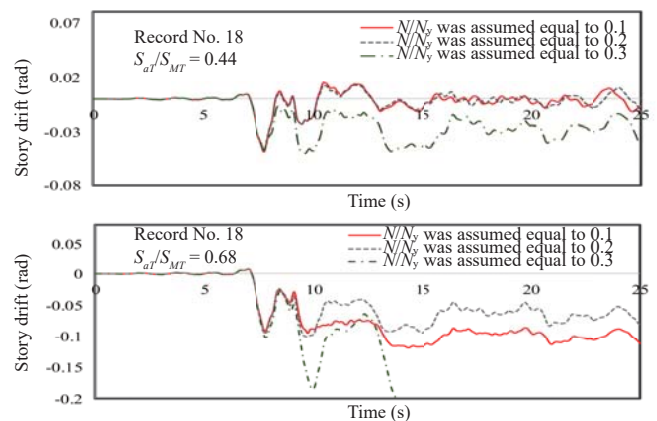

Fig. 12 Different time-histories obtained for Model CPH as the modelling parameters were evaluated for different ratios of presumed axial force in columns to their yield capacity (N/N_y)

the three frame models provided for the SMF archetype. Median collapse capacity is defined as the ground motion intensity under which half of the records in the set cause collapse of an intended frame model. In this study, this intensity was obtained by scaling up the set of 44 individual records until the intended numerical model collapsed under at least 22 records. Vamvatsikos and Cornell (2002) have suggested some criteria to capture the structural collapse from the results of nonlinear dynamic analysis. According to their suggestion, the collapse point is reached when the local tangent of the relevant IDA curve reduces less than 20% of the initial slope of this curve, or when the maximum interstory drift ratio exceeds 10% (0.1 rad). The median collapse capacity obtained for each frame model is represented by a horizontal dashed line in Fig. 13. The collapse margin ratio (CMR) was then assessed by dividing the evaluated $\hat{S}_{CT}$ to the value of S_{MT} calculated for the 6-story SMF archetype. Larger values of CMRs represent lower probability of collapse for the frame under investigation. This index has been generally used in previous research studies in order to evaluate the seismic performance of different lateral load resisting systems (FEMA, 2009; Denavit *et al.*, 2016; Farahi and Mofid, 2013; Nobahar *et al.*, 2016).

CMR ratios evaluated in this study were utilized in order to investigate how the result of a general collapse assessment of a typical SMF can be affected by employing different modelling techniques to simulate the seismic behavior of column members. Collapse margin

ratios were obtained as equal to 3.1, 3.4 and 1.6 for frame models FB-FLPH, FB-DP and CPH, respectively. It can be inferred from these values that the collapse probability of a moment frame can be underestimated if the columns of this frame are modelled using the FB-DP modelling approach compared with the case in which FB-FLPH method is used. Although the deterioration in the seismic behavior of the columns was not taken into account in frame model FB-DP, The difference between the CMRs obtained for this frame model and frame model FB-FLPH is not very significant. However, it should be noted that this index was assessed based on the maximum values captured for the intended structural demand (interstory drift ratio) under the seismic records. In some time-history responses, the most severe peak in the structural response was captured as the structure underwent inelastic deformation for the first time, and before that the response of the intended frame model could even be in the elastic range. Hence, in such cases, the deteriorations in the seismic behavior of structural members could not significantly affect the maximum value for the seismic demand of the interest. On the other hand, the collapse probability of a moment frame can be overestimated if the CPH modelling approach is used to model the frame columns and the required modelling parameters are evaluated assuming a high constant axial force demand on the columns. Note that Lignos and Krawinkler (2009) used the results of the experiments to calibrate Eq. (3) in which column specimens were subjected to constant levels of axial compressive load up

(a) Frame model FB-FLPH

(b) Frame model FBDP
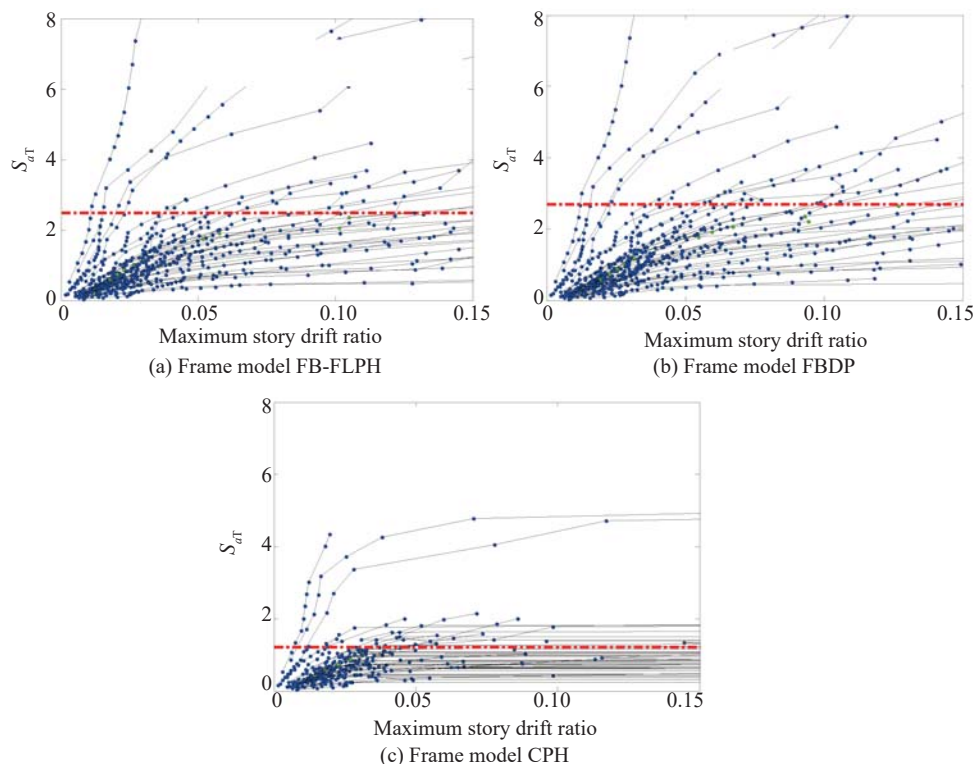
(c) Frame model CPH

Fig. 13 Results of incremental dynamic analyses conducted on the three different numerical models provided for the selected SMF (Horizontal dashed line represent the obtained value for $\hat{S}_{CT}$)

to 40% of their axial yield capacity. However, the level of axial force in columns fluctuates during a seismic event and it may reach very high levels in only a few seconds (Farahi and Erfani, 2016).

It has been shown that the capability of the numerical approach implemented to model the columns of a lateral load resisting frame affects the behavior that is predicted for these members. In addition, it also affects the seismic behavior that is captured for other structural components of the intended frame. Figure 14 shows the rotation time-histories of the same plastic hinges in all the intended frame models. The selected plastic hinge is the left zero-length hinge of the left beam in the first level. As it is apparent from this figure, the rotation time-histories obtained for the same plastic hinge in the three intended frame models deviated from each other. As mentioned before, all the modelling details were the same in the three frame models provided for the SMF archetype except the modelling techniques used to simulate the behavior of the columns. Accordingly, the beams were modelled using the same concentrated plastic hinges at their ends in frame models CPH, FB-FLPH, and FB-DP. Hence, the difference in the beam rotation time-histories can only be attributed to the different accuracy of the modelling techniques used to model the column members in different frame models.

Note that the elongation of column members can be significant during severe ground motions. The axial deformation of columns cannot be simulated numerically if the CPH modelling technique is employed to simulate the seismic behavior of columns. However, both FB-FLPH and FB-DP models are capable of capturing the axial deformations of columns. The axial deformation time-histories obtained for the column in the right side of the first story of both frame models FB-FLPH and FB-PH are shown in Fig. 15. Apparently, a significant

axial deformation was observed for the column as the selected SMF were subjected to record No. 16.

The modelling techniques which are employed to simulate the nonlinear behavior of different components of a structural model should not cause any numerical instability during the intended simulations. Furthermore, the computational cost of the intended simulations is an important concern when different modelling techniques are chosen for different components of a structural model. In the FB-DP modelling procedure, member forces are calculated by referring to section resultant forces at numbers of integration points along the member, and the section behavior can be nonlinear at any integration point. However, in the FB-FLPH method, the section behavior can be nonlinear only at two integration points at the beginning and end of the member (Farahi and Erfani, 2017). In the CPH modelling procedure, member forces are calculated based on a pre-defined phenomenological relation assigned to the end zero-length hinges (nonlinear springs). Hence, employing the fiber-based distributed plasticity approach for modelling columns notably increase the duration of the dynamic analysis compared with the other two approaches. On the contrary, employing the end concentrated plastic hinges expedites the simulations. Note that the simulations were conducted only on a mid-rise 2-D frame in this study. Thus, all the nonlinear dynamic analyzes were completed in a very short time, and the simulation time was not a concern. Accordingly, a quantitative comparison was not provided in this study. However, the difference between simulation times using different modelling techniques would be a concern if the behavior of a large or high-rise 3-D building is intended to be investigated.

On the other hand, divergence issues were raised in some analyses conducted on the frame model CPH, especially when the seismic records were scaled up to high intensities. The time-history analysis conducted on the models in which the FB-FLPH approach was used to model the column members were numerically more
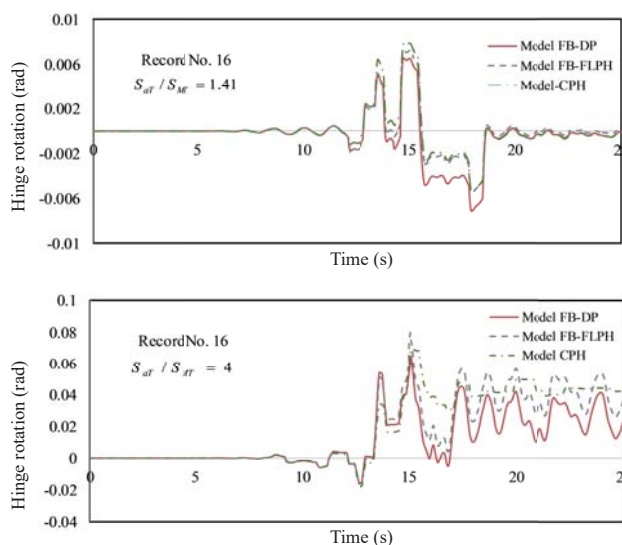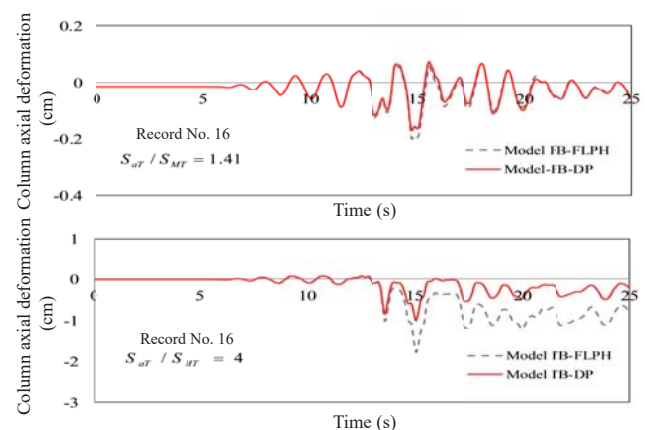

Fig. 14 Rotation time-histories obtained for the left zero-length hinge of the left beam in the first level of each model under record No. 16 scaled to 2 different intensities

Fig. 15 Axial deformation time-histories obtained for the column in the right side of the first story of both Model FB-FLPH and Model FB-PH under record No. 16 scaled to 2 different intensities

stable than the analyses performed on the model with concentrated plastic hinges (frame model CPH). The seismic response of the frame model FB-FLPH was simulated under the seismic records without numerical instabilities even up to collapse limit states (maximum story drift ratios up to 10%). Moreover, the duration of the simulations performed on frame model FB-FLPH did not significantly exceed the duration of the simulations conducted on frame model CPH. Hence, among the three selected modelling techniques, the FB-FLPH modelling technique calibrated in this study was the most efficient model that was used to simulate the seismic behavior of the steel column members.

4   Summary and conclusion

The sufficiency of three different modelling techniques that can be employed to simulate the nonlinear behavior of columns has been investigated in this study. It has also been investigated how the results of the dynamic nonlinear analysis conducted on a typical mid-rise special moment frame can be affected by implementing these different modelling approaches to model the column members of that frame. Three different models were provided for a typical 6-story SMF. In each frame model, one of the intended modelling techniques was employed to model the column members. Subsequently, numerous time-history analyses were carried out on these models under several ground motion records. The simulations conducted on the frame model in which the FB-DP modelling technique had been employed were more time-consuming compared with the relevant simulations performed on the other frame models. In these simulations, the drift story demands in the frame sample were also underestimated compared with the other simulations. The results of these simulations deviated more from the results of other simulations as the residual seismic demands in the frame sample were considered as the target outputs. On the other hand, the results obtained for the frame model in which the CPH modelling technique was employed were dependent on the level of axial force in columns presumed during the evaluation of the required modelling parameters. Since the axial force demand on columns would be notably various during different seismic events, the results of the simulations is not objective if this modelling technique is used to simulate the behavior of the columns. On the other hand, in addition to cyclic deterioration, the calibrated FB-FLPH model is capable of taking into account the P-M interaction taking advantage of fiber discretization. Furthermore, the modelling parameters required for this model depend only on geometric and material properties of the columns and do not depend on any presumed seismic demand. Hence, it has been proved that FB-FLPH modelling approach is the most efficient and accurate way to simulate the seismic and cyclic behavior of steel hollow columns compared with the other modelling approaches employed in this study.

References

ASCE (2010), *ASCE/SEI 7-10: Minimum Design Loads for Buildings And Other Structures*, American Society of Civil Engineering.

AISC (2010), *ANSI/AISC-360-10: Specification for Structural Steel Buildings*, American Institute of Steel Construction, Chicago, Illinois.

AISC (2010), *ANSI/AISC 340-10: Seismic Provisions for Structural Steel Buildings*, American Institute of Steel Construction, Chicago, Illinois.

Bosco M, Ferrara GAF, Ghersi A, Marino EM and Rossi PP (2015), "Predicting Displacement Demand of Multi-Storey Asymmetric Buildings by Nonlinear Static Analysis and Corrective Eccentricities," *Engineering Structures*, **99**(Supplement C): 373–387.

Cheng X, Chen Y and Nethercot DA (2013), "Experimental Study on H-Shaped Steel Beam-Columns with Large Width-Thickness Ratios under Cyclic Bending about Weak-Axis," *Engineering Structures*, **49**: 264–274.

Coleman J and Spacone E (2001), "Localization Issues in Force-Based Frame Elements," *Journal of Structural Engineering-Asce*, **127**(11): 1257–1265.

Del Carpio RM, Mosqueda G and Lignos DG (2016), "Seismic Performance of a Steel Moment Frame Subassembly Tested from the Onset of Damage through Collapse," *Earthquake Engineering & Structural Dynamics*, **45**(10): 1563–1580.

Denavit MD, Hajjar JF, Leon RT and Perea T (2015), "Advanced Analysis and Seismic Design of Concrete-Filled Steel Tube Structures," *Structures Congress*, Proceedings,972–983.doi:10.1061/9780784479117.083.

Denavit MD, Hajjar JF, Perea T and Leon RT (2016), "Seismic Performance Factors for Moment Frames with Steel-Concrete Composite Columns and Steel Beams," *Earthquake Engineering & Structural Dynamics*, **45**(10): 1685–1703.

Eletrabi H and Marshall JD (2015), "Catenary Action in Steel Framed Buildings with Buckling Restrained Braces," *Journal of Constructional Steel Research*, **113**(Supplement C): 221–233.

Farahi M and Mofid M (2013), "On the Quantification of Seismic Performance Factors of Chevron Knee Bracings, in Steel Structures," *Engineering Structures*, **46**: 155–164.

Farahi M and Erfani S (2016), "Developing Representative Dual Loading Protocols for the Columns of Steel Special Moment Frames based on the Seismic Demands on These Members," *Journal of Earthquake Engineering*, **21**(8):1283–1304.

Farahi M and Erfani S (2017), "Employing a Fiber-Based Finite-Length Plastic Hinge Model for Representing the Cyclic and Seismic Behavior of Hollow Steel Columns," *Journal of Steel and Composite Structures*, **23**(5): 501–516.

FEMA P695 (2009), *Quantification of Building Seismic Performance Factors*, Federal Emergency Management Agency, Washington D.C.

Fenves GL and McKenna F (2007), "Computational Simulation for Earthquake Engineering Research and Practice," *Proceedings of Structural Engineering Research Frontiers*, doi:10.1061/40944(249)27.

Filippou FC, Popov EP, and Bertero, VV (1983), "Effects of Bond Deterioration on Hysteretic Behavior of Reinforced Concrete Joints," *UCB/EERC 83-19*, Earthquake Engineering Research Center, Berkeley, California.

Freeman SA (2000), "Performance-Based Seismic Engineering: Past, Current, and Future," *Proceedings of Advanced Technology in Structural Engineering Congress*, doi:10.1061/40492(2000)124.

Fu F (2009), "Progressive Collapse Analysis of High-Rise Building with 3-D Finite Element Modeling Method," *Journal of Constructional Steel Research*, **65**(6): 1269–1278.

Hall JF and Challa VRM (1995), "Beam-Column Modeling," *Journal of Engineering Mechanics*, **121**(12): 1284–1291.

Hamidia M, Filiatrault A and Aref A (2014), "Simplified Seismic Sidesway Collapse Analysis of Frame Buildings," *Earthquake Engineering & Structural Dynamics*, **43**(3): 429–448.

Ibarra LF, Medina RA and Krawinkler H (2005), "Hysteretic Models That Incorporate Strength and Stiffness Deterioration," *Earthquake Engineering & Structural Dynamics*, **34**(12): 1489–1511.

Ikeda K, Mahin SA and Dermitzakis SN (1984), "Phenomenological Modeling of Steel Braces under Cyclic Loading," *UCB/EERC-84/09*, Earthquake Engineering Research Center, Berkeley, California.

Imanpour A, Tremblay R, Davaran A, Stoakes C and Fahnestock LA (2016), "Seismic Performance Assessment of Multitiered Steel Concentrically Braced Frames Designed in Accordance with the 2010 AISC Seismic Provisions," *Journal of Structural Engineering*, **142**(12): 04016135.

Jin J and El-Tawil S (2003), "Inelastic Cyclic Model for Steel Braces," *Journal of Engineering Mechanics*, **129**(5): 548–557.

Kanvinde A, Higgins P, Cooke R, Perez J and Higgins J (2014), "Column Base Connections for Hollow Steel Sections: Seismic Performance and Strength Models," *Journal of Structural Engineering*, **141**(7): 04014171.

Karamanci E and Lignos DG (2014), "Computational Approach for Collapse Assessment of Concentrically Braced Frames in Seismic Regions," *Journal of Structural Engineering*, **140**(8): A4014019.

Kawaguchi J and Morino S (2001), "Experimental Study on Post Local Buckling Behavior of Beam-Columns under Cyclic Loading," *Journal of Structural Construction Engineering*, **540**: 141–148.

Khatib F, Mahin SA and Pister KS (1988), "Seismic Behavior of Concentrically Braced Steel Frames," *UCB/EERC-88/01*, Earthquake Engineering Research Center, University of California, Berkeley, California.

Kurata M, Nakashima M and Suita K (2005), "Effect of Column Base Behavior on the Seismic Response of Steel Moment Frames," *Journal of Earthquake Engineering*, **9**(2): 415–438.

Lignos D and Krawinkler H (2009), "Sidesway Collapse of Deteriorating Structural Systems Under Seismic Excitation," *Rep. No. TR172*, John A. Blume Earthquake Engineering Center, Department of Civil Engineering, Stanford University, Stanford, California.

Lignos DG and Krawinkler H (2011), "Deterioration Modeling of Steel Components in Support of Collapse Prediction of Steel Moment Frames under Earthquake Loading," *Journal of Structural Engineering*, **137**(11): 1291–1302.

Menegotto M and Pinto PE (1973), "Method of Analysis for Cyclically Loaded Reinforced Concrete Plane Frames Including Changes in Geometry and Non-Elastic Behavior of Elements under Combined Normal Force and Bending," *Symposium on the Resistance and Ultimate Deformability of Structures Acted on by Well Defined Repeated Loads, International Association for Bridge and Structural Engineering*, Zurich, Switzerland: 15–22.

Miyamura T, Yamashita T, Akiba H and Ohsaki M (2015), "Dynamic FE Simulation of Four-Story Steel Frame Modeled by Solid Elements and Its Validation Using Results of Full-Scale Shake-Table Test," *Earthquake Engineering & Structural Dynamics*, **44**(9): 1449–1469.

Nakashima M and Liu D (2005), "Instability and Complete Failure of Steel Columns Subjected to Cyclic Loading," *Journal of Engineering Mechanics*, **131**(6): 559–567.

Nobahar E, Farahi M and Mofid M (2016), "Quantification of Seismic Performance Factors of the Buildings Consisting of Disposable Knee Bracing Frames," *Journal of Constructional Steel Research*, **124**: 132–141.

Open System for Earthquake Engineering Simulation (OpenSees) [Computer software], *OpenSees*, Berkeley, California.

Salawdeh S and Goggins J (2013), "Numerical Simulation for Steel Brace Members Incorporating a Fatigue Model," *Engineering Structures*, **46**: 332–349.

Scott MH and Fenves GL (2006), "Plastic Hinge Integration Methods for Force-Based Beam-Column Elements," *Journal of Structural Engineering-Asce*, **132**(2): 244–252.

Scott MH and Hamutçuoğlu OM (2008), "Numerically Consistent Regularization of Force-Based Frame Elements," *International Journal for Numerical Methods*

in Engineering, **76**(10): 1612–1631.

Tzimas AS, Kamaris GS, Karavasilis TL and Galasso C (2016), "Collapse Risk and Residual Drift Performance of Steel Buildings Using Post-Tensioned MRFs and Viscous Dampers in Near-Fault Regions," *Bulletin of Earthquake Engineering*, **14**(6): 1643–1662.

Ucak A and Tsopelas P (2014), "Load Path Effects in Circular Steel Columns under Bidirectional Lateral Cyclic Loading," *Journal of Structural Engineering*, **141**(5): 04014133.

Uriz P, Filippou FC and Mahin SA (2008), "Model for Cyclic Inelastic Buckling of Steel Braces," *Journal of Structural Engineering-Asce*, **134**(4): 619–628.

Vamvatsikos D and Cornell CA (2002), "Incremental Dynamic Analysis," *Earthquake Engineering & Structural Dynamics*, **31**(3): 491–514.